ARAŞTIRMA MAKALESİ / RESEARCH ARTICLE

Magnetic Resonance and Diffusion-weighted Imaging Characteristics of Abdominal Wall Endometriosis: A Cross-sectional Study

Abdominal Duvar Endometriozisinin Manyetik Rezonans ve Difüzyon Ağırlıklı Görüntüleme Özellikleri: Kesitsel Bir Çalışma

Nisa Baspinar[1], Mehmet H. Atalar[1], Serdar Akti[1], Canver Onal[2], Ali Cetin[3]

[1]Department of Radiology, Sivas Cumhuriyet University Faculty of Medicine, Sivas; [2]Department of Radiology, Kafkas University Faculty of Medicine, Kars; [3]Department of Obstetrics and Gynecology, Haseki Training and Research Hospital, University of Health Sciences, Istanbul, Türkiye

ABSTRACT

Aim: *To characterize magnetic resonance imaging (MRI) and diffusion-weighted imaging (DWI) of histologically confirmed abdominal wall endometriosis (AWE) lesions and investigate the potential role of apparent diffusion coefficient (ADC) measurements in preoperative diagnosis.*

Materials and Methods: *This retrospective cross-sectional study included twenty-four women aged 24–44 years with histologically confirmed AWE. Magnetic resonance imaging protocols included T1-weighted, T2-weighted, fat-suppressed contrast-enhanced sequences, and DWI (b-values: 50, 400, 800 sec/mm²). Apparent diffusion coefficient values were measured for AWE lesions and the normal rectus abdominis muscle. Magnetic resonance imaging signal characteristics, enhancement patterns, and quantitative ADC values were analyzed.*

Results: *The endometrial lesions on the abdominal wall appeared predominantly heterogeneous or slightly hyperintense on the T2-weighted images and were isointense or slightly hyperintense on the T1-weighted images. Patchy T1-hyperintense hemorrhagic foci were observed in 70.8% of cases. Quantitative analysis of diffusion-weighted imaging showed that the mean ADC value of the AWE lesions ($1.19 \pm 0.26 \times 10^{-3}$ mm²/sec) was significantly lower than that of the normal rectus abdominis muscle ($1.32 \pm 0.20 \times 10^{-3}$ mm²/sec). The difference between the two groups was statistically significant ($p=0.042$).*

Conclusion: *MRI in combination with DWI provides valuable morphologic and microstructural information for the evaluation of AWE. Apparent diffusion coefficient measurements can serve as supportive parameters in preoperative assessment, although further comparative studies with other abdominal wall masses are warranted.*

Key words: *abdominal wall; diffusion-weighted imaging; endometriosis; magnetic resonance imaging*

ÖZET

Amaç: *Histolojik olarak doğrulanmış abdominal duvar endometriozisi (AWE) lezyonlarının manyetik rezonans görüntüleme (MRG) ve difüzyon ağırlıklı görüntüleme (DAG) ile karakterize edilmesi ve görünür difüzyon katsayısı (ADC) ölçümlerinin preoperatif tanıdaki potansiyel rolünün araştırılması.*

Gereç ve Yöntem: *Bu retrospektif kesitsel çalışmaya, yaşları 24–44 arasında değişen ve histopatolojik olarak AWE tanısı konmuş 24 kadın dâhil edildi. Manyetik rezonans görüntüleme protokolleri; T1 ağırlıklı, T2 ağırlıklı, yağ baskılı kontrastlı sekanslar ve DAG (b-değerleri: 50, 400, 800 s/mm²) içermekteydi. Abdominal duvar endometriozisi lezyonları ve normal rektus abdominis kası için ADC değerleri ölçüldü. Manyetik rezonans görüntüleme sinyal özellikleri, kontrast tutulum paternleri ve kantitatif ADC değerleri analiz edildi.*

Bulgular: *Abdominal duvardaki endometriozis lezyonları, T2 ağırlıklı görüntülerde çoğunlukla heterojen veya hafif hiperintens; T1 ağırlıklı görüntülerde ise izointens veya hafif hiperintens olarak izlendi. Vakaların %70,8'inde düzensiz T1-hiperintens hemorajik odaklar gözlendi. Difüzyon ağırlıklı görüntülemenin kantitatif analizinde, AWE lezyonlarının ortalama ADC değeri ($1{,}19 \pm 0{,}26 \times 10^{-3}$ mm²/sn), normal rektus abdominis kasının ortalama ADC değerinden ($1{,}32 \pm 0{,}20 \times 10^{-3}$ mm²/sn) anlamlı düzeyde düşük bulundu ($p=0{,}042$).*

Sonuç: *MRG ile birlikte kullanılan DAG, AWE'nin değerlendirilmesinde değerli morfolojik ve mikroyapısal bilgiler sağlar. Görünür difüzyon katsayısı ölçümleri, preoperatif değerlendirmede destekleyici parametreler olarak kullanılabilir; ancak, diğer abdominal duvar kitleleri ile karşılaştırmalı ileri çalışmalara ihtiyaç vardır.*

Anahtar kelimeler: *abdominal duvar; difüzyon ağırlıklı görüntüleme; endometriozis, manyetik rezonans görüntüleme*

İletişim/Contact: *Nisa Başpınar, Department of Radiology, Sivas Cumhuriyet University Faculty of Medicine, Sivas, Türkiye* • ***Tel:*** *0530 075 82 42* • ***E-mail:*** *nisabozbiyik@yahoo.com* • ***Geliş/Received:*** *22.11.2025* • ***Kabul/Accepted:*** *05.02.2026*

ORCID: *Nisa Başpınar: 0000-0003-4240-6001 • Mehmet H. Atalar: 0000-0003-3076-8072 • Serdar Aktı: 0000-0002-7934-7730 • Canver Önal:0000-0001-6797-2574 • Ali Çetin: 0000-0002-5767-7894*

Introduction

Abdominal wall endometriosis (AWE) is a distinct pathological entity characterized by functional endometrial tissue within the abdominal wall, most commonly occurring after gynecologic surgical procedures, particularly cesarean sections (1,2). The pathogenesis of AWE involves a combination of mechanical, hormonal, and inflammatory mechanisms. During surgical interventions, direct implantation of endometrial cells along the surgical tract may occur, followed by estrogen-dependent proliferation and chronic inflammatory response within the abdominal wall layers (2–5). Clinically, AWE typically presents as a palpable, firm mass located at or near the surgical scar and is often associated with localized pain that may show cyclical exacerbation during the menstrual cycle. However, continuous pain can also be observed (1–4). Notably, symptom severity does not necessarily correlate with lesion size, as even small lesions may cause significant discomfort due to involvement of adjacent fascia, muscle, or nerve endings (1–4).

Endometriosis remains a challenging gynecological condition affecting women of reproductive age, with varying presentations and locations throughout the body. Abdominal wall endometriosis (AWE), a specific form of extrapelvic endometriosis, most commonly occurs following cesarean sections or other gynecological procedures. The increasing prevalence of AWE, particularly amid rising cesarean section rates worldwide, necessitates improved diagnostic approaches to identify and manage it (2–6) accurately.

Magnetic resonance imaging (MRI) has emerged as a valuable diagnostic tool for evaluating AWE, offering superior soft-tissue contrast and multiplanar imaging capabilities. The addition of diffusion-weighted imaging (DWI) to conventional MRI protocols provides further diagnostic information by characterizing tissue cellularity and microstructural properties. However, the specific imaging characteristics of AWE on MRI and DWI have not been fully elucidated in larger patient cohorts (7–8).

Although ultrasound is the primary imaging modality for suspected AWE due to its availability and high sensitivity, MRI provides superior tissue contrast and lesion-marginal delineation. The addition of diffusion-weighted imaging (DWI) may offer further diagnostic value by characterizing microstructural features, potentially assisting in differential diagnosis and preoperative planning**.**

In the present study, the MRI and DWI characteristics of abdominal wall endometriosis were investigated in 24 patients.

This comprehensive imaging analysis aims to establish reliable diagnostic criteria and enhance our understanding of the radiological features of AWE, potentially improving preoperative diagnosis and surgical approach.

Materials and Methods

Study Population

We present here twenty-four patients with abdominal wall endometriosis (AWE) diagnosed by MRI. In addition to MRI, DWI was also included in the diagnosis. Twenty-four women aged 24–44 years were included in the study. The patients had a total of twenty-four AWE lesions. Three patients had no history of surgery or interventions. Two patients had undergone diagnostic laparoscopy previously. All other patients had a history of gynecologic surgery. In 14 patients, an ultrasound examination (US) performed before MRI revealed a mass on the anterior abdominal wall suspicious for AWE. Magnetic resonance images of all patients were also examined for deep infiltrating endometriosis, endometrioma, and adenomyosis. The diagnosis of AWE was confirmed by histopathological assessment in all but three patients.

Magnetic Resonance Imaging Technique and Image Analysis

Magnetic resonance imaging of the pelvis was performed with a 1.5 Tesla scanner (Magnetom Aera, Siemens Healthcare, Erlangen, Germany). Size, location, and MRI appearance of lesions were recorded on T1-weighted (T1W), T2-weighted (T2W), and post-contrast fat-suppressed (FS) T1W images. An intravenous contrast agent (gadoteric acid) was used. Diffusion-weighted imaging was also performed in all patients. The DWI examination was performed before the contrast agent was administered. Apparent diffusion coefficient values were calculated with b-values of 50, 400, and 800 sec/mm^2.

For quantitative analysis, a region of interest (ROI) of at least 10 mm^2 was placed in the solid, most homogeneous part of the lesion, avoiding necrotic, cystic, or hemorrhagic areas. In each lesion, three separate ROIs were measured, and the mean ADC value was calculated. In addition, the ADC values of the normal-appearing rectus abdominis muscle were measured at the level of the lesion in all patients. Experienced radiologists reviewed all images during imaging of the women.

Statistical Analysis

We collected data about lesion location, lateral position, MRI appearance, contrast enhancement, and ADC values. The data are presented as numbers and percentages. Quantitative data were expressed as mean ± standard deviation. Since the data distribution was confirmed to be normal using the Shapiro–Wilk test, parametric statistical tests were applied. Statistical comparisons between groups were performed using paired sample t-tests to assess differences in ADC values, and Pearson correlation analysis was used to evaluate associations between lesion size and ADC values. A p-value <0.05 was considered statistically significant.

Ethical Considerations

This work was a retrospective observational study approved by the Human Ethics Committee for non-interventional research (Sivas Cumhuriyet University, Registry no: 2021–05/07 dated May 26, 2021).

Results

The study cohort consisted of twenty-four women with a mean age at symptom onset of 32.8±5.06 years (range, 24–44 years). The complaints were a mass in the abdominal wall (n=21), cyclic pain (n=17) and dysmenorrhea (n=15). The AWE lesions were located dorsally or ventrally at the aponeurosis of the rectus abdominis muscle (n=4, 15.4%) (Fig. 1), within the rectus abdominis muscle (n=8, 34.6%) (Fig. 2) and at the incision line (n=12, 50%) (Fig. 3). Three lesions in the aponeurosis of the rectus abdominis muscle were located on the left side and one on the right side. Six of the lesions in the rectus abdominis muscle were located on the right side and two on the left side. The size of the lesions ranged from 13×7 mm to 32×15 mm in the axial plane. The contours of the lesions were generally irregular (65%), but lesions with normal contours were not uncommon (35%). On conventional MRI sequences, the majority of AWE lesions appeared heterogeneous or slightly hyperintense on T2W images compared to adjacent muscle tissue. On T1W images, the lesions were predominantly isointense or mildly hyperintense compared to the muscle. Patchy T1 hyperintense foci suggestive of intralesional hemorrhage were found in 17 of 24 patients (70.8%). Post-contrast T1W FS sequences showed mild to moderate enhancement in most lesions. On diffusion-weighted imaging (DWI), all lesions showed hyperintensity on high

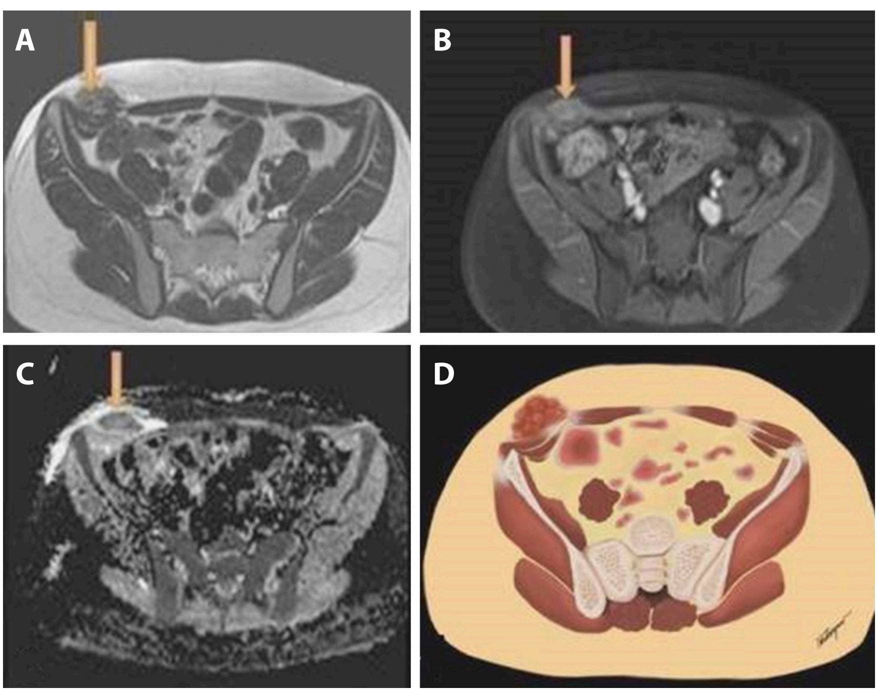

Figure 1. *Magnetic resonance imaging findings of abdominal wall endometriosis in a 29-year-old woman, with the lesion located at the aponeurosis of the right rectus abdominis muscle.* ***(A)*** *Axial T2-weighted image demonstrates a well-defined lesion (arrow) at the right rectus abdominis aponeurosis with intermediate-to-low signal intensity.* ***(B)*** *Axial fat-suppressed T2-weighted image shows heterogeneous high signal intensity within the lesion (arrow), compatible with hemorrhagic content.* ***(C)*** *Axial diffusion-weighted imaging (DWI) and apparent diffusion coefficient (ADC) map reveal restricted diffusion (arrow), supporting the diagnosis of endometriosis.* ***(D)*** *Schematic illustration depicting the typical appearance and location of abdominal wall endometriosis involving the right rectus abdominis aponeurosis.*

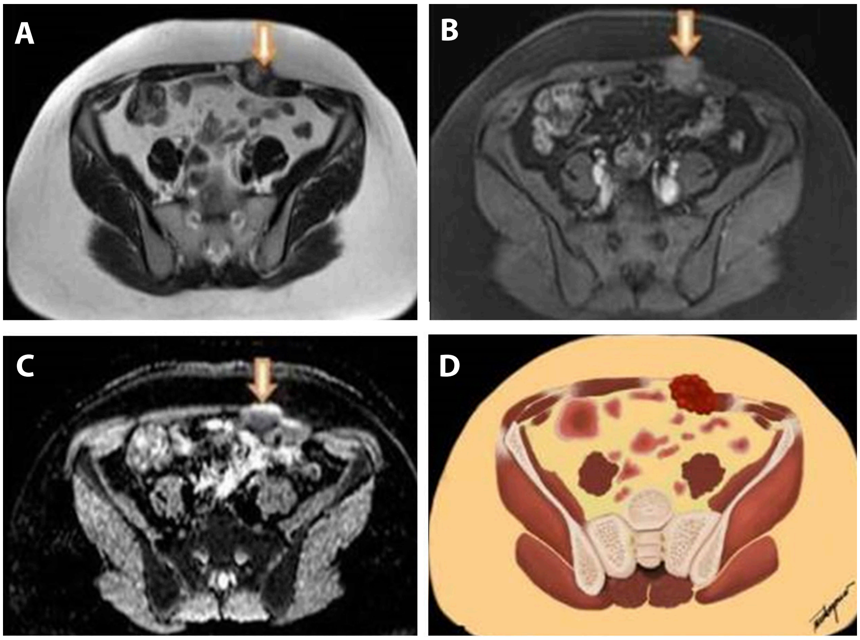

Figure 2. *Magnetic resonance imaging characteristics of abdominal wall endometriosis in a 33-year-old woman, with the lesion located within the left rectus abdominis muscle.* ***(A)*** *Axial T2-weighted image shows a lesion (arrow) involving the left rectus abdominis muscle with predominantly intermediate signal intensity.* ***(B)*** *Axial contrast-enhanced fat-suppressed T1-weighted image demonstrates marked contrast enhancement of the rectus muscle lesion (arrow), indicating vascularity and active inflammatory/hemorrhagic components.* ***(C)*** *Axial apparent diffusion coefficient (ADC) map shows low ADC values within the lesion (arrow), consistent with restricted diffusion typically seen in active endometriotic tissue.* ***(D)*** *Schematic illustration depicting abdominal wall endometriosis involving the left rectus abdominis muscle.*

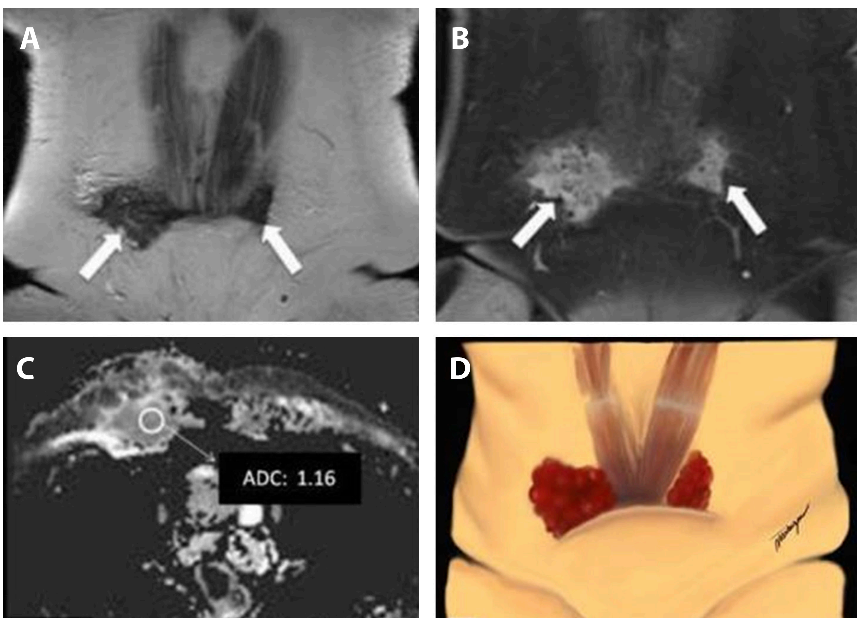

Figure 3. *Magnetic resonance imaging features of bilateral incisional abdominal wall endometriosis in a 33-year-old woman.* ***(A)*** *Coronal T2-weighted image shows bilateral heterogeneous lesions (arrows) located along the anterior abdominal wall incision line.* ***(B)*** *Coronal contrast-enhanced fat-suppressed T1-weighted image demonstrates intense and irregular contrast enhancement of both incision-line lesions (arrows).* ***(C)*** *Axial apparent diffusion coefficient (ADC) map shows low ADC values (1.16×10^{-3} mm^2/s), consistent with restricted diffusion typical of active endometriosis.* ***(D)*** *Schematic illustration depicting bilateral endometriotic nodules situated along the surgical incision line of the anterior abdominal wall.*

b-value images (b=800 sec/mm^2). The mean ADC value for AWE lesions was calculated as $1.19 \pm 0.26 \times 10^{-3}$ mm^2/sec (Fig. 4a), whereas the mean ADC value for normal rectus abdominis muscle was $1.32 \pm 0.20 \times 10^{-3}$ mm^2/sec (Fig. 4b). A paired sample t-test demonstrated that the ADC values of AWE lesions were significantly lower compared to normal muscle tissue ($p=0.042$). Pearson correlation analysis did not reveal a statistically significant association between lesion size and ADC values ($p > 0.05$). Normality testing with the Shapiro–Wilk test confirmed that the data were normally distributed, supporting the use of parametric analyses. For each lesion, three separate ROI measurements (=10 mm^2) were obtained, and the mean ADC value was used for statistical evaluation. Subgroup analysis of ADC values by lesion localization did not reveal statistically significant differences, which may be attributable to the limited sample size. Ten of the 24 patients had pelvic endometriosis detected at different locations on MRI. The average ADC values according to the localization of the lesions are shown in Figure 4 c. Pelvic endometriosis detected on MRI did

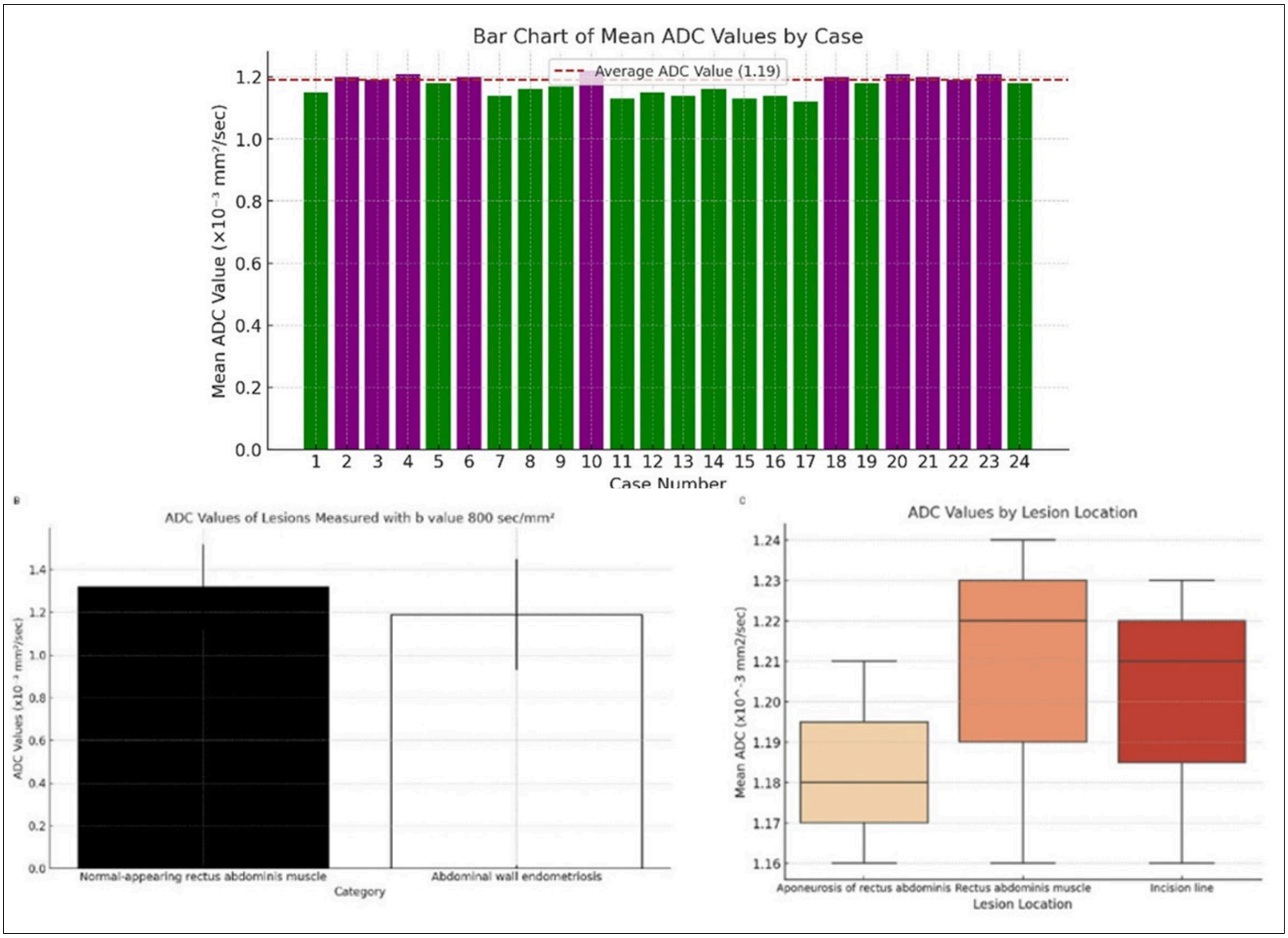

Figure 4. ***(A)*** *Mean apparent diffusion coefficient (ADC) values (×10⁻³ mm²/s) of abdominal wall endometriosis lesions in 24 cases, with individual lesion measurements and the overall cohort mean (1.19).* ***(B)*** *ADC values (b=800 sec/mm²) in normal rectus abdominis muscle and abdominal wall endometriosis lesions.* ***(C)*** *Mean apparent diffusion coefficient (ADC) values (×10⁻³ mm²/s) of abdominal wall endometriosis lesions according to anatomical location.*

not appear to significantly influence the imaging characteristics of the abdominal wall endometriosis lesions in this cohort. The clinical and radiologic features of the patients are listed in Table 1.

Discussion

The incidence of endometriosis after a cesarean section was reported to be 0.26% over a period of 25 years (9). A similar incidence was reported in another study by Singh et al. (10). The literature reports an average time from cesarean section to symptom onset of 3.7–4.5 years. The disease is characterized by a triad of an abdominal wall mass, cyclic pain, and a history of abdominal surgery (3). Bacanakgil et al. (4) reported a history of previous cesarean section in 63 of 66 cases in their study of AWE. The most common symptoms in the patients were pain and a palpable mass. In a series of 83 patients, Benedetto et al. reported secondary endometriotic implants after cesarean section in 55 cases. Cyclic abdominal wall pain was the most common complaint, occurring in 60 patients. The second most common complaint was a mass in the abdominal wall. In our study, the most common complaint was a mass in the abdominal wall (21 cases), followed by cyclic pain (17 cases). In the present study, we presented twenty-four cases of AWE in twenty-four patients.

Abdominal wall endometriosis, a subtype of non-pelvic endometriosis, accounts for 4% of all cases of external endometriosis. Abdominal wall endometriosis is usually found in the skin and subcutaneous tissue, but occurs mainly in the incisional scar and in the umbilical region. It is rarely seen in the inguinal canal or rectus abdominis muscles. Abdominal wall endometriosis should be considered in the differential diagnosis of anterior abdominal wall masses in women of childbearing age, particularly if symptoms recur with each menstrual cycle. Various imaging techniques, such as ultrasound, computed tomography, and MRI, are used

Table 1. The patient's clinical and radiological characteristics

Case no	Age (year)	Clinical presentation	History of cesarean section	Pfannenstiel incision	Location	T1/T2W signal intensity	Gd-enhancement	Mean ADC value (x10^{-3} mm^2/sec)
1	38	Abdominal wall mass, cyclic pain	-	-	Right rectus muscle	Hypointense / Heterogeneous	Moderate	1.15
2	26	Abdominal wall mass, cyclic pain	-	-	Left rectus aponeurosis	Hypointense / Heterogeneous	Mild	1.18
3	33	Cyclic pain, dysmenorrhea	-	-	Right rectus muscle	Hyperintense / Heterogeneous	Moderate	1.20
4	29	Abdominal wall mass, dysmenorrhea	2	+	Right rectus aponeurosis	Hypointense / Heterogeneous	Mild	1.21
5	33	Abdominal wall mass, cyclic pain, dysmenorrhea	2	+	Incision line	Hypointense / Heterogeneous	Moderate	1.19
6	26	Abdominal wall mass, cyclic pain	1	+	Incision line	Iso- or hyper-intense	Moderate	1.20
7	24	Abdominal wall mass, cyclic pain	1	+	Incision line	Hypointense / Heterogeneous	Mild	1.18
8	44	Abdominal wall mass, cyclic pain	3	+	Incision line	Iso- or hyper-intense	Moderate	1.16
9	29	Abdominal wall mass, dysmenorrhea	2	+	Incision line	Hypo- or hyper-intense	Mild	1.21
10	30	Cyclic pain, dysmenorrhea	-	-	Left rectus muscle	Hypointense / Heterogeneous	Moderate	1.22
11	33	Abdominal wall mass, cyclic pain	2	+	Left rectus muscle	Hypointense / Heterogeneous	Mild	1.19
12	36	Abdominal wall mass	2	+	Left rectus aponeurosis	Hypointense / Heterogeneous	Moderate	1.18
13	34	Dysmenorrhea	1	+	Incision line	Iso- or hyper-intense	Mild	1.15
14	38	Abdominal wall mass, cyclic pain, dysmenorrhea	2	+	Incision line	Iso- or hyper-intense	Moderate	1.16
15	34	Abdominal wall mass, cyclic pain	-	-	Left rectus muscle	Hyper- / Heterogeneous	Moderate	1.18
16	35	Abdominal wall mass, cyclic pain, dysmenorrhea	2	+	Incision line	Iso- or hyper-intense	Moderate	1.24
17	33	Abdominal wall mass, dysmenorrhea	1	+	Right rectus muscle	Hypo- or hyper-intense	Mild	1.15
18	34	Abdominal wall mass, cyclic pain, dysmenorrhea	1	+	Right rectus aponeurosis	Hypointense / Heterogeneous	Moderate	1.18
19	42	Abdominal wall mass, dysmenorrhea	2	+	Incision line	Hypo- or hyper-intense	Moderate	1.20
20	37	Abdominal wall mass, cyclic pain, dysmenorrhea	1	+	Incision line	Hypo- or hyper-intense	Moderate	1.23
21	24	Abdominal wall mass, dysmenorrhea	1	+	Right rectus muscle	Hypo- or hyper-intense	Mild	1.21
22	32	Abdominal wall mass, cyclic pain	1	+	Incision line	Hypointense / Heterogeneous	Mild	1.22
23	33	Abdominal wall mass, cyclic pain	2	+	Incision line	Hypointense / Heterogeneous	Moderate	1.22
24	31	Abdominal wall mass, cyclic pain	1	+	Right rectus muscle	Hypo- or hyper-intense	Moderate	1.17

T1W: T1-weighted; T2W: T2-weighted; Gd: gadolinium; ADC: apparent diffusion coefficient.

to assess AWE. In particular, MRI findings may vary depending on the menstrual cycle, disease duration, amount of implanted tissue, amount of bleeding, and presence of concomitant inflammation. It is recommended that imaging examinations be preferably performed during the menstrual cycle (5,6,10).

Abdominal wall endometriosis lesions show isointense or slightly hyperintense signals compared to muscle on MRI T2W images and are isointense or slightly hyperintense signals compared to muscle on T1W images. Foci with high signal intensity on T1W images indicate hemorrhage (11,12). In the present study, the typical appearance of almost all lesions on MR images was iso-hyperintense on T1W, hyperintense-heterogeneous on T2W, and focal hyperintense spots (due to hemorrhage) on T1W-FS series. Most lesions had irregular margins, indicating the infiltrative nature of AWE. After gadolinium contrast injection, the lesions showed mild to moderate contrast enhancement.

In our study, the mean ADC value was $1.19 \pm 0.26 \times 10^{-3}$ mm^2/s. Busard et al. (12) conducted a study of ten patients with AWE in which the location of the lesions and the depth of infiltration were assessed using magnetic resonance imaging (MRI). Lesions typically appeared isointense or hyperintense on T2W images, with foci of high signal intensity, and isointense or slightly hyperintense on T1W images with fat suppression. The mean ADC value of five AWE lesions was 0.93×10^{-3} mm^2/sec (range: $0.79–1.10 \times 10^{-3}$ mm^2/sec), suggesting that DWI may help distinguish AWE from other abdominal wall masses. In the study by Franz et al. (13), the mean ADC value for four AWEs was 1.25×10^{-3} mm^2/sec. Genc et al. (14) found that mean ADC values for AWEs vary with the phases of the menstrual cycle. In their study, ADC measurements were significantly lower during the menstrual phase than during the luteal phase (menstrual phase: $0.93 \pm 0.25 \times 10^{-3}$ mm^2/sec; luteal phase: $1.25 \pm 0.21 \times 10^{-3}$ mm^2/sec). Hu et al. (15) investigated the diagnostic performance of MRI in combination with ultrasound-guided high-intensity focused ultrasound (USg-HIFU) in AWE. The study found that MRI provided clearer images for detecting AWE lesions than color Doppler ultrasound, particularly for determining lesion size and borders. Magnetic resonance imaging features of AWE lesions included mixed, isointense, or slightly hypointense signals on T1W images and hypointense to mixed signals on T2W images. They concluded that MRI is valuable in the diagnosis and treatment planning of AWE. In their study, the mean ADC value of AWE lesions before treatment was 1.47×10^{-3} mm^2/s. Differences in ADC values may be related to variations in menstrual cycle phases. The ADC values in AWE are compared in Table 2.

In the differential diagnosis of AWE, diagnoses such as abscess, desmoid tumor, lipoma, liposarcoma, hematoma, and primary and metastatic cancer are often included (2,6,16). Desmoid tumors of the abdominal wall, in particular, are the most common masses that can be confused radiologically with AWE. In a recent study, the mean ADC value of a desmoid tumor of the abdominal wall was $1.72 \pm 0.13 \times 10^{-3}$ mm^2/sec (17). Lower ADC values of abdominal wall endometriosis compared with other abdominal wall masses, such as desmoid tumors, may contribute to differential diagnosis.

Table 2. *Literature comparison of ADC values in endometriosis of the abdominal wall*

Study	Number of cases	Mean ADC value ($\times 10^{-3}$ mm^2/sec)	ADC value range ($\times 10^{-3}$ mm^2/sec)
Busard et al. (2010)	5	0.93	0.79–1.10
Franz et al. (2014)	4	1.25	Not applicable
Genc et al. (2014)			
Menstrual phase	10	0.93	0.68–1.18
Luteal phase	10	1.25	1.04–1.46
Hu et al. (2022)	30	1.47	1.20–1.59

In this study, we investigated the imaging characteristics of AWE using MRI and DWI, which showed different signal intensities and ADC values. Our results are consistent with previous studies and emphasize the utility of advanced imaging techniques for the accurate diagnosis of AWE. However, several limitations must be considered to provide a comprehensive perspective in this study. The study included only 24 patients, which limits the statistical power and generalizability of the results. As AWE is a rare condition, small cohorts are common in the literature; nevertheless, larger, multicenter studies are required. The retrospective design may have introduced selection bias and variability in imaging protocols. Hormonal changes during the menstrual cycle significantly affect the imaging features of endometriotic lesions, including ADC values. Another limitation of this study is that the patients' menstrual cycle phases at the time of imaging were not recorded, which may have influenced ADC measurements. Although Genc et al. (14) have shown that ADC values vary with menstrual phases, our study did not consider the timing of imaging relative to patients' menstrual cycles, which could affect the consistency of the results. In addition, the absence of a direct comparison with other common abdominal wall masses, such as desmoid tumors, hematomas, or soft-tissue sarcomas, may have limited the specificity of the imaging findings.

This absence of a control group limits the specificity of our findings. Such comparisons could improve understanding of the imaging features that differentiate AWE and increase diagnostic specificity. Although the diagnosis was confirmed by histopathological examination in most cases, three patients did not undergo surgical excision. This reliance on imaging alone may have led to diagnostic inaccuracies in these cases. Postoperative outcomes and recurrence rates were not examined in this study. Long-term follow-up would provide valuable insight into the prognosis of AWE and the role of imaging in surveillance for recurrence. This study was conducted at a single institution, which may limit the external validity of the results. Imaging equipment and expertise may vary across centers, which could affect the reproducibility of results.

Although ultrasound remains the first-line imaging modality due to its high sensitivity and specificity, MRI provides superior soft-tissue contrast and better delineation of lesion margins, depth of infiltration, and relationships with adjacent structures, which are crucial for surgical planning (7,8,12,15). Diffusion-weighted imaging further contributes by characterizing microstructural tissue properties and may assist in differentiating AWE from desmoid tumors or other soft-tissue masses (12,17). In addition, MRI findings such as lesion size, depth, and fascial or muscular involvement may guide the surgical approach, ensuring complete excision and reducing the risk of recurrence (5,9,15).

However, the routine use of MRI and DWI in all suspected cases of AWE is not cost-effective. Instead, a stepwise diagnostic algorithm in which ultrasound is used as the initial modality and MRI/DWI is reserved for inconclusive cases or preoperative mapping may represent the most practical and economically feasible approach (7,10,15). The addition of diffusion-weighted imaging provides complementary microstructural information beyond conventional MRI, supporting lesion characterization in abdominal wall endometriosis. Apparent diffusion coefficient measurements may contribute to preoperative assessment and surgical planning by improving lesion delineation and supporting differential diagnosis.

References

1. Grigore M, Sokolov D, Pavaleanu I, Scripcariu I, Grigore AM, Micu R. Abdominal wall endometriosis: an update in clinical, imagistic features, and management options. Med Ultrason. 2017;19:430–437. https://doi.org/10.11152/mu-1248
2. Foley CE, Ayers PG, Lee TT. Abdominal wall endometriosis. Obstet Gynecol Clin North Am. 2022;49:369–380. https://doi.org/10.1016/j.ogc.2022.02.013
3. Thanasa A, Thanasa E, Antoniou IR, Kontogeorgis G, Gerokostas EE, Kamaretsos E, et al. Abdominal wall endometriosis: early diagnosis of a rare iatrogenic complication following cesarean section. Cureus. 2024;16:e56284. https://doi.org/10.7759/cureus.56284
4. Bacanakgil BH, Özçam H, Deveci M, Yıldırım SG. Abdominal wall endometriosis: analysis of 66 patients at a tertiary center. Istanbul Med J. 2019;20(2):94–97. https://doi.org/10.4274/imj.galenos.2018.50490
5. Benedetto C, Cacozza D, de Sousa Costa D, Coloma Cruz A, Tessmann Zomer M, Cosma S, et al. Abdominal wall endometriosis: report of 83 cases. Int J Gynaecol Obstet. 2022;159:530–536. https://doi.org/10.1002/ijgo.14167
6. Bozkurt M, Cil AS, Bozkurt DK. Intramuscular abdominal wall endometriosis treated by ultrasound-guided ethanol injection. Clin Med Res. 2014;12:160–165. https://doi.org/10.3121/cmr.2013.1183
7. Gidwaney R, Badler RL, Yam BL, Hines JJ, Alexeeva V, Donovan V, et al. Endometriosis of abdominal and pelvic wall scars: multimodality imaging findings, pathologic correlation, and radiologic mimics. Radiographics. 2012;32:2031–2043. https://doi.org/10.1148/rg.327125024
8. Stein L, Elsayes KM, Wagner-Bartak N. Subcutaneous abdominal wall masses: radiological reasoning. AJR Am J Roentgenol. 2012;198:W146–W151. https://doi.org/10.2214/AJR.10.7238
9. Nominato NS, Prates LF, Lauar I, Morais J, Maia L, Geber S. Caesarean section greatly increases risk of scar endometriosis. Eur J Obstet Gynecol Reprod Biol. 2010;152:83–85. https://doi.org/10.1016/j.ejogrb.2010.05.001
10. Singh KK, Lessells AM, Adam DJ, Jordan C, Miles WF, Macintyre IM, et al. Presentation of endometriosis to general surgeons: a 10-year experience. Br J Surg. 1995;82:1349–1351. https://doi.org/10.1002/bjs.1800821017
11. Jaramillo-Cardoso A, Balcacer P, Garces-Descovich A, Beker K, Roth E, Glickman J, et al. Multimodality imaging and clinicopathologic assessment of abdominal wall endometriosis: knocking down the enigma. Abdom Radiol (NY). 2020;45:1800–1811. https://doi.org/10.1007/s00261-018-1666-1
12. Busard MP, Mijatovic V, van Kuijk C, Hompes PG, van Waesberghe JH. Appearance of abdominal wall endometriosis on MR imaging. Eur Radiol. 2010;20:1267–1276. https://doi.org/10.1007/s00330-009-1658-1
13. Franz M, Klotz T, Montoriol PF, Garcier JM, Canis M, Da Ines D; Clermont-Ferrand/FR. Abdominal wall endometriosis: MRI features of 31 lesions with histological confirmation. ECR 2014; C–1798. https://doi.org/10.1594/ecr2014/C-1798
14. Genc B, Solak A, Sahin N, Genç M, Ogul H, Sivrikoz ON, et al. Diffusion-weighted imaging in the evaluation of hormonal cyclic changes in abdominal wall endometriomas. Clin Radiol. 2014;69:130–136. https://doi.org/10.1016/j.crad.2013.08.015
15. Hu S, Liu Y, Chen R, Xiao Z. Exploring the diagnostic performance of magnetic resonance imaging in ultrasound-guided high-intensity focused ultrasound ablation for abdominal wall endometriosis. Front Physiol. 2022;13:819259. https://doi.org/10.3389/fphys.2022.819259
16. Ballard DH, Mazaheri P, Oppenheimer DC, Lubner MG, Menias CO, Pickhardt PJ, et al. Imaging of abdominal wall masses, mass-like lesions, and diffuse processes. Radiographics. 2020;40:684–706. https://doi.org/10.1148/rg.2020190170
17. Khanna M, Ramanathan S, Kambal AS, Al-Berawi M, Yadav S, Kumar D, et al. Multi-parametric MRI for the diagnosis of abdominal wall desmoid tumors. Eur J Radiol. 2017;92:103–110. https://doi.org/10.1016/j.ejrad.2017.04.010